Polyhedron xxx (2014) xxx–xxx

Contents lists available at ScienceDirect

Polyhedron

journal homepage: www.elsevier.com/locate/poly

Synthesis, structure, characterization and study of antiproliferative activity of dimeric and tetrameric oxidomolybdenum(VI) complexes of *N*,*N*′-disalicyloylhydrazine

Sagarika Pasayat [a], Subhashree P. Dash [a], Sudarshana Majumder [a], Rupam Dinda [a,*], Ekkehard Sinn [b], Helen Stoeckli-Evans [c], Subhadip Mukhopadhyay [d], Sujit K. Bhutia [d], Partha Mitra [e]

[a] Department of Chemistry, National Institute of Technology, Rourkela 769008, Odisha, India
[b] Department of Chemistry, Western Michigan University, Kalamazoo, MI 49008, USA
[c] Institute of Physics, University of Neuchâtel, Rue Emile-Argand 11, CH-2000 Neuchâtel, Switzerland
[d] Department of Life Science, National Institute of Technology, Rourkela 769008, Odisha, India
[e] Department of Inorganic Chemistry, IACS Kolkata, Kolkata 700032, West Bengal, India

ARTICLE INFO

Article history:
Received 10 December 2013
Accepted 4 April 2014
Available online xxxx

Keywords:
N,*N*′-Disalicyloylhydrazine
Oxidomolybdenum(VI)
Dimeric and tetrameric complexes
X-ray crystal structure
Antiproliferative activity

ABSTRACT

The *in situ* reaction of salicyloylhydrazide and its corresponding hydrazone with $[MoO_2(acac)_2]$ afforded two novel and unusual dimeric $[(Mo^{VI}O_2)_2L]$ (**1**) and tetrameric $[\{(C_2H_5OH)LO_3Mo_2^{VI}\}_2(\mu\text{-}O)_2]\cdot C_2H_5OH$ (**2**) oxidomolybdenum(VI) complexes with *N*,*N*′-disalicyloylhydrazine (H_2L). The binucleating ligand was formed by the self-combination of the acid hydrazide or corresponding hydrazone. The complexes were characterized by various spectroscopic techniques (IR, UV and NMR) and also by electrochemical study. The molecular structures of both complexes have been confirmed by X-ray crystallography. The above studies indicate that the *N*,*N*′-disalicyloylhydrazine (H_2L) has the normal tendency to form both dimeric and tetrameric complexes coordinated through the dianionic tridentate manner. The *in vitro* antiproliferative activity of complexes **1** and **2** was assayed against HeLa cell line.

1. Introduction

Molybdenum(VI) complexes have attracted considerable interest due to their relevance to the active sites of the majority of molybdo-enzymes [1,2]. Oxo-peroxo and dioxo complexes of Mo(VI) with polydentate nitrogen, sulfur and oxygen ligands are considered valuable models for the active site of several Mo enzymes. Recent discovery of the antitumor effects of metal complexes and their potential use in cancer diseases have received increasing attention [3–10].

Some molybdenum complexes, particularly, thiosemicarbazonato molybdenum(VI) complexes [11] have been found to possess antitumor activity. Yamase et al. have reported the antitumoral effect of polyoxomolybdates, especially $[NH_3Pr^i]_6[Mo_7O_{24}]\cdot 3H_2O$ (PM-8) against MX-1 murine mammary cancer cell line, Meth A sarcoma and MM46 adenocarcinoma [12]. Cindrić et al. showed that γ-octamolybdates containing aminoacids and peptides showed differential cell-growth inhibition in a dose-dependent manner selectively on hepatocellular carcinoma cell line (HepG2) and breast cancer cell line (MCF-7) [13]. Recently, some new molybdenum η3-allyldicarbonyl complexes $[Mo(\eta3\text{-}C_3H_5)Br(CO)_2(L)]$ and $[\{Mo(\eta3\text{-}C_3H_5)Br(CO)_2\}_2(\mu\text{-}L)]$ with the bidentate nitrogen ligands (L) were reported [14] to exhibit potent antitumor activity against HeLa cell line. A. Scorilas and co-workers [15] described the cytotoxic activity of some 2,5-dihydroxybenzoate molybdenum(VI) with tetraphenylphosphonium as counter ion against two human leukaemia cell lines HL-60 and K562. Bandarra et al. have reported [16] the *in vitro* cytotoxic activity of some molybdenum(II) complexes $[Mo(\eta3\text{-}C_3H_5)(CF_3SO_3)(CO)_2(N\text{-}N)]$ against human cancer cell lines cervical carcinoma (HeLa) and breast carcinoma (MCF-7). Very recently, Gleeson et al. [17] have reported the cytotoxicity studies of three molybdocene dichloride derivatives against the human renal cell line Caki-1.

On the other hand, hydrazones, –NH–N = CRR′ (R and R′ = H, alkyl, aryl), are versatile ligands due to their applications in the field of analytical [18] and medicinal chemistry [19–21]. Hydrazone moieties are the most important pharmacophoric cores of several anticancer, antiinflammatory, antinociceptive, and antiplatelet drugs [22–29]. In the context of the present study it is relevant to mention that although the chemistry of dioxidomolybdenum(VI)-aroylhydrazone complexes is well

* Corresponding author. Tel.: +91 661 246 2657; fax: +91 661 246 2022.
E-mail address: rupamdinda@nitrkl.ac.in (R. Dinda).

http://dx.doi.org/10.1016/j.poly.2014.04.007
0277-5387/

developed [30–36], to the best of our knowledge no information is available concerning their anticancer properties.

However, the research on the compounds with symmetrical diaroylhydrazine ligands is limited [37–42]. The *N*,*N*′-diacylhydrazines have value as structural components of heterocyclic ring systems [43], and as tuberculostatic agents [44]. The *N*,*N*′-disalicyloylhydrazine [45], which had previously been known to chelate a variety of metal ions [45,46], has been shown to exhibit potent inhibition of the human immune deficiency virus (HIV) integrase [47].

In our effort to discover and develop apoptosis inducers as potential new anticancer agents, we recently synthesized [48] three highly stable, hexacoordinated nonoxidovanadium(IV), $V^{IV}(L)_2$, complexes of sterically constrained hydrazone ligands and found that these compounds could inhibit proliferation of HeLa cells. Here in, we report the synthesis, structure and characterization of two new dimeric $[(Mo^{VI}O_2)_2L]$ (**1**) and tetrameric $[\{(C_2H_5OH)LO_3Mo_2^{VI}\}_2(\mu\text{-}O)_2]\cdot C_2H_5OH$ (**2**) oxidomolybdenum(VI) complexes synthesized from the same ligand, *N*,*N*′-disalicyloylhydrazine along with special reference to their antiproliferative activities.

2. Experimental

2.1. Materials

$[MoO_2(acac)_2]$ and salicyloylhydrazide were prepared as described in the literature [49,50]. Reagent grade solvents were dried and distilled prior to use. All other chemicals were reagent grade, available commercially and used as received. Commercially available TBAP (tetrabutylammonium perchlorate) was properly dried and used as a supporting electrolyte for recording cyclic voltammograms of the complexes.

2.2. Physical measurements

Elemental analyses were performed on a Vario ELcube CHNS Elemental analyzer. IR spectra were recorded on a Perkin-Elmer Spectrum RXI spectrometer. ^{1}H NMR spectra were recorded with a Bruker Ultrashield 400 MHz spectrometer using $SiMe_4$ as an internal standard. Electronic spectra were recorded on a Lamda25, PerkinElmer spectrophotometer. Magnetic susceptibility was measured with a Sherwood Scientific AUTOMSB sample magnetometer. Electrochemical data were collected using a PAR electrochemical analyzer and a PC-controlled Potentiostat/Galvanostat (PAR 273A) at 298 K in a dry nitrogen atmosphere. Cyclic voltammetry experiments were carried out with a platinum working electrode, platinum auxiliary electrode, Ag/AgCl as reference electrode and TBAP as supporting electrolyte.

2.3. Synthesis of 2-hydroxybenzoylhydrazone of acetophenone

The ligand 2-hydroxybenzoylhydrazone of acetophenone was prepared by the condensation of equimolar ratio of salicyloylhydrazide 2.72 g (20.00 mmol) and acetophenone 2.38 g (20.00 mmol) in stirring ethanol (25 ml) for 2 h following a standard procedure [51]. The resulting yellowish-white compound was filtered, washed with ethanol and dried over fused $CaCl_2$. Yield: 0.18 g (75%). *Anal.* Calc. for $C_{15}H_{14}N_2O_2$: C, 70.88; H, 5.55; N, 11.08. Found: C, 70.90; H, 5.54; N, 11.06%. ^{1}H NMR (400 MHz, DMSO-d_6): δ = 11.83 (s, 1H, OH), 11.35 (s, 1H, NH), 8.03–6.97 (m, 9H, Aromatic), 2.33 (s, 3H, CH_3),.^{13}C NMR (DMSO-d_6, 100 MHz): δ = 164.99, 159.50, 157.99, 149.49, 134.44, 132.08, 129.04, 128.83, 126.89, 119.85, 119.08, 117.77, 116.92, 116.06, 14.34.

2.4. Synthesis of complex $[(Mo^{VI}O_2)_2L]$ (**1**)

To the refluxing solution of 0.15 g (1.0 mmol) of salicyloylhydrazide in 30 mL of ethanol 0.32 g (1.0 mmol) of $MoO_2(acac)_2$ was added [52]. The color of the solution changed to dark red. The mixture was then refluxed for 3 h. After leaving the solution for 2 days at room temperature, fine dark red colored crystals were isolated and a suitable single crystal was selected for X-ray analysis. *$[(Mo^{VI}O_2)_2L]$ (**1**):* Yield: 0.36 g (68%). *Anal.* Calc. for $C_{14}H_8N_2O_8Mo_2$: C, 32.08; H, 1.53; N, 5.34. Found: C, 32.06; H, 1.55; N, 5.37%. ^{1}H NMR (DMSO-d_6, 400 MHz): δ = 7.94–7.02 (m, 4H, Aromatic). ^{13}C NMR (DMSO-d_6, 100 MHz): δ = 163.55, 162.00, 135.42, 129.87, 122.53, 120.03, 115.80.

2.5. Synthesis of complex $[\{(C_2H_5OH)LO_3Mo_2^{VI}\}_2(\mu\text{-}O)_2]\cdot C_2H_5OH$ (**2**)

0.24 g (1.00 mmol) of 2-hydroxybenzoylhydrazone of acetophenone was dissolved in 30 mL ethanol. When 0.32 g (1.00 mmol) of $MoO_2(acac)_2$ was added to the solution, the color changed to dark orange [51].The solution mixture was then refluxed for 3 h. After leaving the solution for 2 days at room temperature, fine dark orange crystals were isolated and a suitable single crystal was selected for X-ray analysis. *$[\{(C_2H_5OH)LO_3Mo_2^{VI}\}_2(\mu\text{-}O)_2]\cdot C_2H_5OH$ (**2**):* Yield: 0.19 g (73%). *Anal.* Calc. for $C_{36}H_{40}N_4O_{20}Mo_4$: C, 35.06; H, 3.27; N, 4.55. Found: C, 35.08; H, 3.25; N, 4.56%. ^{1}H NMR (DMSO-d_6, 400 MHz): δ = 8.14–7.06 (m, 8H, Aromatic), 4.36 (s, 1H, OH), 3.42 (q, 2H, CH_2), 1.05 (s, 3H, CH_3). ^{13}C NMR (DMSO-d_6, 100 MHz): δ = 163.58, 163.46, 162.42, 162.02, 135.58, 134.67, 129.87, 128.69, 122.67, 121.22, 120.10, 118.87, 115.67, 114.96, 56.49,55.95, 19.10, 19.00.

2.6. Crystallography

The X-ray diffraction data and unit cell parameters for single crystals of complexes **1** and **2** were collected at 293(2) K, on a Bruker Smart Apex CCD diffractometer using graphite monochromated Mo Kα radiation (k = 0.71073 Å), employing the ω–2θ scan technique. The intensity data were corrected for Lorentz, polarization and absorption effects. The structures were solved with SHELXS*97* [53] and refined with SHELXL*97* [53]. The H-atoms were included in calculated positions and treated as riding atoms using SHELXL default parameters. The non-H atoms were refined anisotropically, using weighted full-matrix least-squares on F^2. Further crystallographic data and refinement details are given in Table 1. The molecular structures and crystal packing of the two complexes are illustrated in the Figs. 2–5 drawn with Mercury [54].

2.7. Cytotoxic assay

HeLa (human cervical carcinoma cells) were obtained from National Centre of Cell Science (NCCS), Pune, India and were maintained in minimal essential medium supplemented with 10% fetal bovine serum, penicillin streptomycin solution and incubated at 37 °C in 5% CO2 and 95% humidified incubator. HeLa cells were harvested from maintenance cultures in logarithmic phase, after counting in a hemocytometer using trypan blue solution. The cell concentration was adjusted to 5x10^4 cells/ml and the cells were plated in a 96 well flat bottom culture plate and incubated for 72 h with various concentrations of the test compounds which were dissolved in a 90% (v/v) DMF solution. The effect of the drugs on the cancer cell viability was studied using MTT dye reduction assay by measuring the optical density at 595 nm using microplate reader spectrophotometer (Perkin–Elmer 2030) [55]. DMF solution that was used to dissolve the drugs was used in control group treatment. MTT (yellow colored) enters the living cells' mitochondria where mitochondrial succinate dehydrogenase

Table 1
Crystal and refinement data of complexes **1** and **2**.

Compound	**1**	**2**
Formula	$C_{14}H_8Mo_2N_2O_8$	$C_{36}H_{40}Mo_4N_4O_{20}$
M	524.10	1232.50
Crystal symmetry	triclinic	triclinic
Space group	$P\bar{1}$	$P\bar{1}$
a (Å)	3.96540(10)	9.5892(3)
b (Å)	9.5080(2)	10.7151(4)
c (Å)	10.1683(2)	11.4986(4)
α (°)	76.167(10)	68.042(10)
β (°)	87.856(10)	73.353(10)
γ (°)	82.230(10)	81.152(2)
V (Å^3)	368.834(14)	1048.39(6)
Z	1	1
D_{calc} (g cm^{-3})	2.360	1.952
$F(000)$	254	612
μ(Mo Kα) (mm^{-1})	1.753	1.256
2θ (max) (°)	26.37	25.50
Reflections collected/ unique	11936/1498	9430/3870
R_1[a] [$I > 2\sigma(I)$]	R_1 = 0.0224, wR_2 = 0.0782	R_1 = 0.0413, wR_2 = 0.0790
wR_2[b] (all data)	R_1 = 0.0214, R_2 = 0.0815	R_1 = 0.0285, wR_2 = 0.0736
S (goodness of fit)	0.793	1.062
Min./max. res. (e Å^{-3})	0.843/−0.649	0.920/−0.873

[a] $R_1 = \sum|F_O| - |F_C|/\sum|F_O|$.
[b] $wR_2 = \{\sum[w(F_O^2 - F_C^2)^2]/\sum[w(F_O^2)^2]\}^{1/2}$.

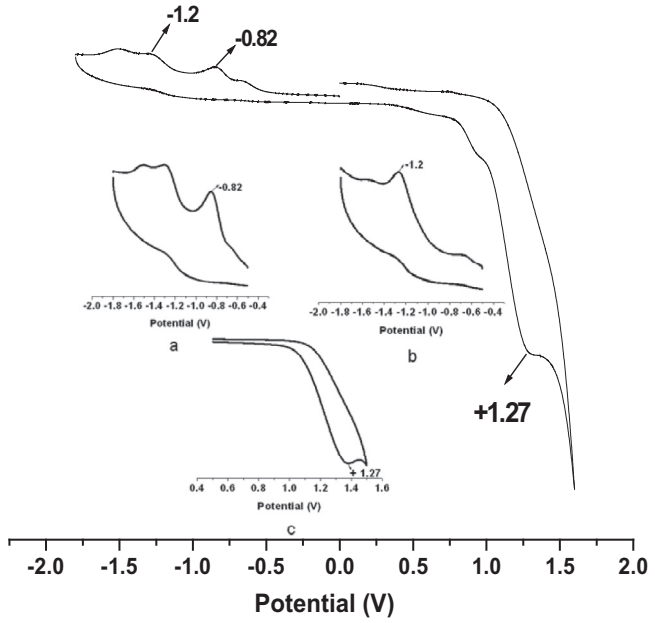

Fig. 1. Cyclic voltammogram of [(Mo^{VI}O$_2$)$_2$L] (**1**) in DMSO showing (a) reduction of (Mo(VI)→Mo(V)), (b) reduction of (Mo(V) → Mo(IV)) and (c) oxidation of ligand.

reduces MTT to produce the insoluble purple colored formazan. Only living cells are able to reduce MTT. This formazan is solubilised by DMSO in order to quantify (spectrophotometrically) the viable number of cellular population that could survive the drug insult.

2.8. Nuclear staining

Nuclear staining using DAPI stain was performed according to the method previously described [56]. Briefly, HeLa cells either treated or untreated with test compounds were smeared on a clean glass slide, cells were fixed with 3.7% formaldehyde for 15 min., permeabilized with 0.1% Triton X-100 and stained with 1 μg/ml DAPI for 5 min at 37 °C. The cells were then washed with PBS (phosphate buffer saline) and examined by fluorescence microscopy (Olympus IX 71) to determine condensation or fragmentation of the nuclei indicating cells undergoing apoptosis. Normal cells display a round uniform margin whereas drug induced apoptosis initiates chromatin condensation and membrane blebbing. Hence drug treated cells with condensed chromatin display a broken margin which is a characteristic phenotype of cells undergoing apoptosis.

3. Results and discussion

3.1. Synthesis

Scheme 1 summarizes the synthesis of two new dimeric and tetrameric oxidomolybdenum(VI) complexes **1** and **2** from the common ligand, *N*,*N*′-disalicyloylhydrazine (H_2L) employed in the present study. According to the demand, to provide the exact stereo and electronic environment for the stability of well known penta- and hexacoordinated dioxidomolybdenum(VI) complexes, the *N*,*N*′-disalicyloylhydrazine ligand (H_2L) was synthesized by the self-combination of salicyloylhydrazide or its corresponding hydrazone of acetophenone and subsequently transformed to the corresponding oxidomolybdenum(VI) species through *in situ* reaction with metal precursor $MoO_2(acac)_2$. The *in situ* formation of this type of intermediate ligand (H_2L) is a general phenomenon and can be prepared in absence of any basic or acidic condition [57]. There is also report where the reaction is accelerated in presence of acidic [37] and basic [58] medium. In the present report the metal precursor in ethanol may provide the acidic medium (pH 3.5) required for this self-combination.

Methods used for synthesis of the precursor hydrazide, hydrazone and oxidomolybdenum complexes (**1** and **2**) are given in experimental section. Proposed structures of these complexes (Scheme 1) are based on their spectroscopic characterization (IR, electronic and ^{1}H NMR spectroscopy), elemental analyses and single crystal X-ray diffraction studies. The binucleating ligand coordinates through its dianionic $(ONO)^{2-}$ enolate tautomeric forms.

The compounds are highly soluble in aprotic solvents, viz. DMF or DMSO and are sparingly soluble in alcohol, CH_3CN and $CHCl_3$. The complexes are diamagnetic, indicating the presence of molybdenum in the +6 oxidation state.

3.2. Spectral properties

Spectral characteristics of precursor 2-hydroxybenzoylhydrazone of acetophenone and complexes **1** and **2** are listed in Table 2. The IR spectra of complexes exhibit two peaks in the range 1602–1601 cm^{-1} and 1579–1549 cm^{-1} due to ν(C=C/aromatic) and ν(C=N) stretching modes [51] respectively. New bands at 662–644 cm^{-1} are assigned to ν(Mo–N) [59]. In addition, **1** and **2** display strong and a moderately strong band in the range 944–943 cm^{-1} and 921–918 cm^{-1} due to terminal ν(M=O$_t$) stretch [30,33,51]. A strong band at 752 cm^{-1} for complex **2** may be assigned to (Mo–O–Mo) stretch [60].

The DMSO solution of **1** and **2** displays a shoulder in the 426–423 nm region and two strong absorptions are located in the 314–312 nm and 274–260 nm range, which are assignable to L → Mo (dπ) LMCT and intraligand transitions respectively [30,33,51].The above results and absence of low energy transition peaks in UV–Vis spectrum clearly suggest the presence of corresponding Mo(VI) species in solution.

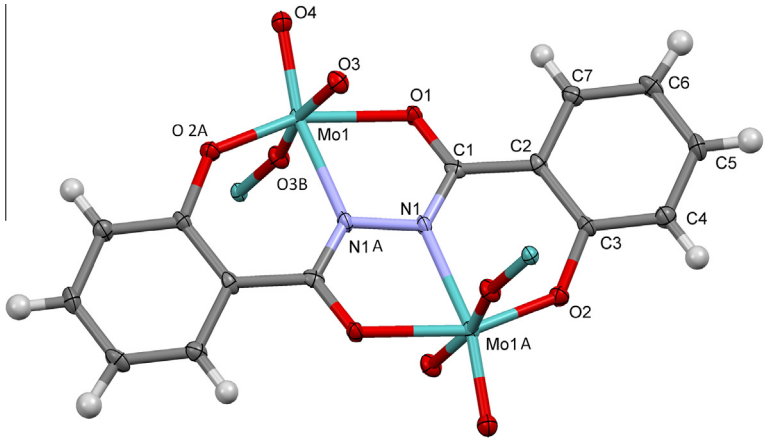

Fig. 2. The molecular structure of $[(Mo^{VI}O_2)_2L]$ (**1**), with atom labeling. Displacement ellipsoids are drawn at the 50% probability level. The molecule possesses inversion symmetry. [symmetry codes: (A) = $-x, -y, -z+1$; (B) $x-1, y, z$].

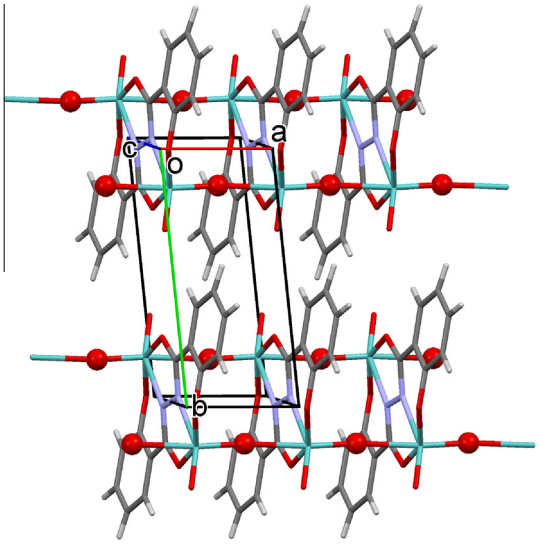

Fig. 3. A view along the *c* axis of the crystal packing of $[(Mo^{VI}O_2)_2L]$ (**1**).

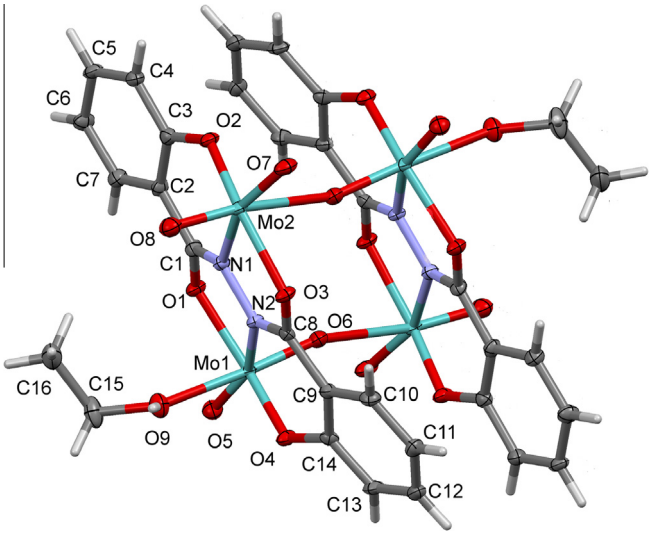

Fig. 4. The molecular structure of $[\{(C_2H_5OH)LO_3Mo_2^{VI}\}_2(\mu\text{-}O)_2]\cdot C_2H_5OH$ (**2**), with atom labeling. Displacement ellipsoids are drawn at the 50% probability level. The molecule possesses inversion symmetry. The ethanol solvent molecule of crystallization has been omitted for clarity.

The ^1H and ^{13}C NMR data of the 2-hydroxybenzoylhydrazone of acetophenone and complexes are given in the experimental section. The spectrum of the hydrazone exhibits an –OH (phenolic) resonance at $\delta = 11.83$ ppm and one –NH proton resonance at $\delta = 11.35$ ppm. All the aromatic proton signals are clearly observed at $\delta = 8.03–6.97$ ppm and the CH_3 proton resonance is observed at $\delta = 2.33$ ppm. In the NMR spectra of complexes (**1** and **2**), the absence of signal due to aromatic –OH indicates that the phenolic group is coordinated to the metal centre after proton replacement. The aromatic protons are observed at $\delta = 8.14–7.02$ ppm [30,33,51]. The chemical shift of the coordinated C_2H_5OH of complex (**2**) exhibits an –OH resonance at $\delta = 4.36$ ppm, $-CH_2$ resonance at $\delta = 3.42$ ppm and $-CH_3$ resonance at $\delta = 1.05$ ppm.

3.3. Electrochemical properties

Electrochemical properties of the complexes were studied by cyclic voltammetry in DMSO solution (0.1 M TBAP). The potential data are listed in Table 3 and Fig. 1 depicts a representative voltammogram of complex **1**. The CV traces of complexes (**1** and **2**) exhibit two irreversible reductive responses within the potential window −0.15 to −0.82 V and −1.06 to −1.2 V, which are assigned to Mo^{VI}/Mo^{V} and Mo^{V}/Mo^{IV} processes respectively [30,33,51]. An oxidation wave at positive potentials in the range of +1.27 to +1.48 V is assigned to the oxidation of the coordinated ligand [61]. As the Mo(VI) complex cannot undergo a metal-centered oxidation, this is attributed to a ligand-centered process [51].

3.4. Description of the X-ray structure of complex $[(Mo^{VI}O_2)_2L]$ (**1**) and $[\{(C_2H_5OH)LO_3Mo_2^{VI}\}_2(\mu\text{-}O)_2]\cdot C_2H_5OH$ (**2**)

The reaction of salicyloylhydrazide and its corresponding hydrazone of acetophenone with the metal precursor does not produce the expected complexes **I** and **II** (Chart 1). However, during *in situ* reaction the hydrazide and its hydrazone were transformed into *N,N′*-disalicyloylhydrazine (**H_2L**), which subsequently reacts with $MoO_2(acac)_2$ and produced two novel bi- and tetranuclear oxidomolybdenum(VI) complexes $[(MoO_2)_2L]$ (**1**) and $[\{(C_2H_5OH)LO_3Mo_2^{VI}\}_2(\mu\text{-}O)_2]\cdot C_2H_5OH$ (**2**), respectively (Scheme 1).

The molecular structure and atom numbering scheme for complex **1** is shown in Fig. 2, with the relevant bond distances and angles collected in Table 4. The molecule possesses inversion symmetry. Each molybdenum atom coordinates with an 'NO_4' chromophore and adopts a distorted tetragonal pyramidal geometry. Both

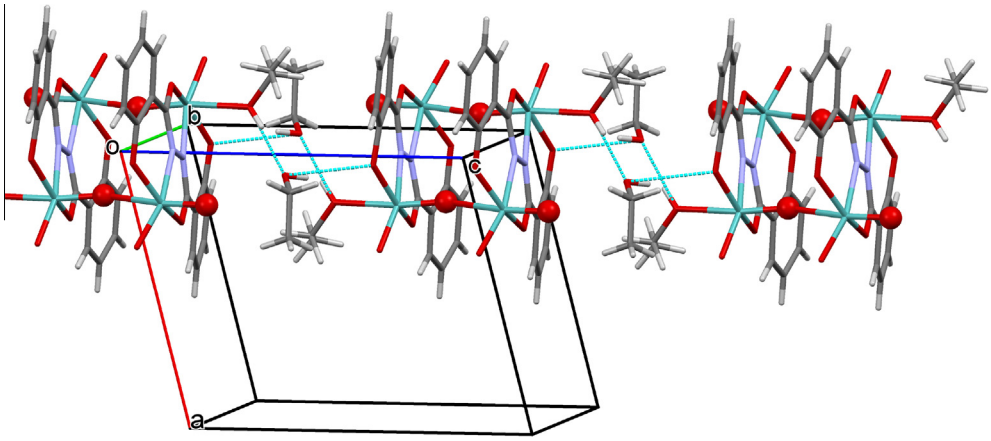

Fig. 5. A view along the *b* axis of the crystal packing of $[\{(C_2H_5OH)LO_3Mo_2^{VI}\}_2(\mu\text{-}O)_2]\cdot C_2H_5OH$ (**2**). The O–H···O hydrogen bonds are shown as dashed lines.

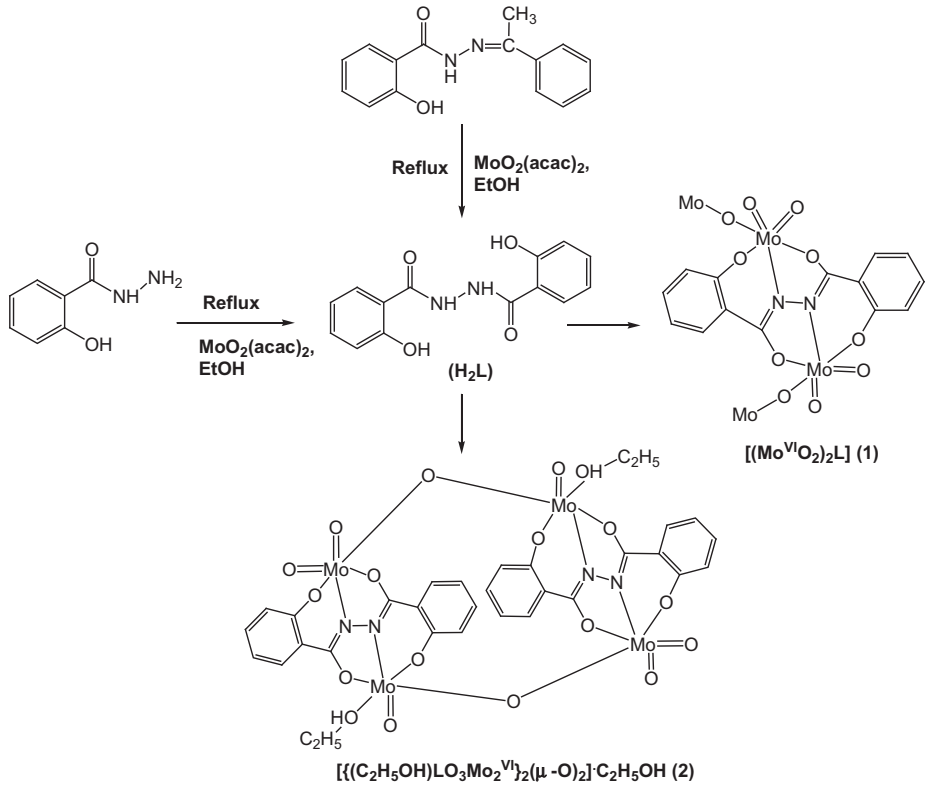

Scheme 1. Schematic representation of synthesis of **1** and **2**.

Table 2
Characteristic IR[a] bands and electronic spectral data[b] for the studied ligand and complexes (**1** and **2**).

Compounds	ν(C=C)	ν(C=N)	ν(Mo=O)ν	(Mo–N)/cm^{-1}	λ_{max}/nm (ε/dm^3 mol^{-1} cm^{-1})
Precursor Ligand	1611	1581	–	–	331 (23524), 292 (15624)
Complex **1**	1602	1579	944, 918	662	426 (9439), 314 (25123), 274 (16352)
Complex **2**	1601	1549	943, 921	644	423 (9569), 312 (26126), 260 (15711)

[a] In KBr pellet.
[b] In DMSO.

sides of the ligand behave as a tridentate (ONO) binegative unit, where one side of the ligand offers two oxygens as donors to the Mo(1) center, one from the enolate oxygen O(1) and the other from the phenolate oxygen O(2), and the last two are oxo O(3) and O(4) atoms with bite angles of 71.90(7) [O(1)–Mo(1)–N(1A)] and 80.50(8) [O(2A)–Mo(1)–N(1A)], forming one five- and one six-membered chelate ring. The planar structure of the chelating groups of ligand **H_2L** in compound **1** favors the delocalization of the double bonds. Hence, bond N(1)–N(1A) = 1.380(3) Å [symmetry code: (A) = *x*, −*y*, −*z* + 1] is shorter than a standard N–N bond

Table 3
Cyclic voltammetric results for oxidomolybdenum(VI) complexes (**1** and **2**) at 298 K.

Complexes	*Epc* [V][a]
Complex **1**	−0.82, −1.2
Complex **2**	−0.15, −1.06

[a] Solvent: DMSO; working electrode: platinum; auxiliary electrode: platinum; reference electrode: Ag/AgCl; supporting electrolyte: 0.1 M TBAP; scan rate: 50 mV/s. *Epc* is the cathodic peak potential.

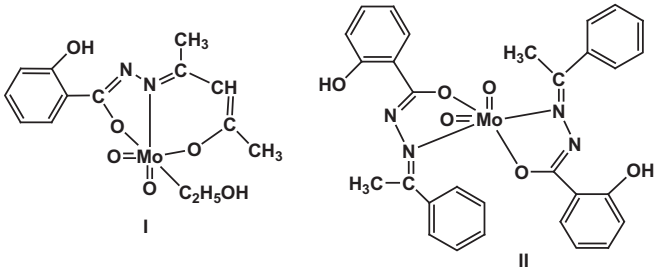

Chart 1. Expected oxidomolybdenum complexes from precursor hydrazide and hydrazone.

Table 4
Selected bond distances (Å) and bond angles (°) for complex **1**.

Distances			
Mo(1)–O(1)	2.037(2)	Mo(1)–O(2A)	1.900(2)
Mo(1)–O(3)	1.728(2)	Mo(1)–O(4)	1.693(2)
Mo(1)–N(1A)	2.211(2)	Mo(1)–O(3B)	2.252(2)
N(1)–N(1A)	1.380(3)	N(1)–C(1)	1.309(3)
Angles			
O(1)–Mo(1)–O(2A)	150.01(8)	O(1)–Mo(1)–O(3)	95.59(9)
O(1)–Mo(1)–O(4)	98.08(11)	O(1)–Mo(1)–N(1A)	71.90(7)
O(2A)–Mo(1)–O(3)	98.85(9)	O(2A)–Mo(1)–O(4)	103.20(9)
O(2A)–Mo(1)–N(1A)	80.50(8)	O(3B)–Mo(1)–O(4)	83.49(9)
O(3)–Mo(1)–N(1A)	96.15(9)	O(4)–Mo(1)–N(1A)	157.24(9)

Symmetry codes: A = $-x$, $-y$, $-z+1$; B = $x-1$, y, z.

distance (1.45 Å) [33]. At the same time, the N(1)–C(1) bond = 1.309(3) Å is shorter than the length of a standard C=N bond (1.34 Å) [45]. The other bond lengths and bond angles in the organic ligands are close to standard values [62].

In the crystal of complex **1**, the binuclear units are linked via bridging Mo···O bonds to form columns propagating along the *a* axis direction (Fig. 3). Actually the sixth coordination site, trans to the oxo-oxygen O(3), is occupied by an oxo-oxygen O(3B) of the next neighboring complex molecule and this pattern is repeated leading to a chain of $[(MoO_2)_2L]$ molecules. This may be visualized as an effect of stacking of the complex molecules along the *a*-axis [30]. The length of the Mo–O(3B) bond (2.252 (2) Å) is considerably longer than the other Mo–O bonds, the longest of which [Mo–O(1)] is 2.037 (2) Å which suggests that this should be explained as oligomeric structure where one of the oxygen of one molybdenum weakly interacts with other.

Reaction of $MoO_2(acac)_2$ with 2-hydroxybenzoylhydrazone of acetophenone lead to the formation of $[\{(C_2H_5OH)LO_3Mo^{VI}_2\}_2(\mu\text{-}O)_2]\cdot C_2H_5OH$ (**2**), a novel di-μ-oxido tetrameric structure, illustrated in Fig. 4. The relevant bond distances and angles are collected in Table 5. The molecular structure of **2** is similar to that of complex **1**; again the molecule possesses inversion symmetry. The two crystallographically equivalent halves are bridged by two oxygen atoms (only the geometry of one half of the complex will be described in detail). Both the Mo centers [Mo(1) and Mo(2)] are six coordinate having an 'NO_5' chromophore, with a distorted octahedral structure. The ligand *N*,*N*'–disalicyloylhydrazine

Table 5
Selected bond distances (Å) and bond angles (°) for complex **2**.

Distances			
Mo(1)–O(1)	2.029(2)	Mo(2)–O(2)	1.920(3)
Mo(1)–O(4)	1.919(3)	Mo(2)–O(3)	2.043(3)
Mo(1)–O(5)	1.692(3)	Mo(2)–O(7)	1.704(3)
Mo(1)–O(6)	1.715(2)	Mo(2)–O(8)	1.694(3)
Mo(1)–O(9)	2.272(3)	Mo(2)–O(6)	2.409(2)
Mo(1)–N(2)	2.204(3)	Mo(2)–N(1)	2.199(3)
Angles			
O(1)–Mo(1)–O(4)	150.1(1)	O(2)–Mo(2)–O(3)	147.9(1)
O(1)–Mo(1)–O(5)	97.2(1)	O(2)–Mo(2)–O(8)	101.4(1)
O(1)–Mo(1)–O(6)	96.1(1)	O(2)–Mo(2)–O(7)	102.0(1)
O(1)–Mo(1)–O(9)	82.2(1)	O(2)–Mo(2)–N(1)	80.3(1)
O(1)–Mo(1)–N(2)	72.3(1)	O(2)–Mo(2)–O(6)	81.1(1)
O(4)–Mo(1)–O(5)	104.3(1)	O(3)–Mo(2)–O(7)	96.8(1)
O(4)–Mo(1)–O(6)	98.0(1)	O(3)–Mo(2)–O(8)	98.2(1)
O(4)–Mo(1)–O(9)	80.5(1)	O(3)–Mo(2)–N(1)	71.8(1)
O(4)–Mo(1)–N(2)	80.2(1)	O(3)–Mo(2)–O(6)	75.92(9)
O(5)–Mo(1)–O(6)	105.2(1)	O(7)–Mo(2)–O(8)	105.6(1)
O(5)–Mo(1)–O(9)	82.1(1)	O(7)–Mo(2)–N(1)	154.4(1)
O(5)–Mo(1)–N(2)	157.5(1)	O(7)–Mo(2)–O(6)	82.1(1)
O(6)–Mo(1)–O(9)	172.6(1)	O(8)–Mo(2)–N(1)	98.8(1)
O(6)–Mo(1)–N(2)	95.8(1)	O(7)–Mo(2)–O(6)	171.0(1)
O(9)–Mo(1)–N(2)	76.8(1)	N(1)–Mo(2)–O(6)	73.0(1)

Symmetry code: (C) = $-x$, $-y$, $-z+2$.

coordinates to the molybdenum in the same manner as in complex **1**. As expected from its structure, the tridentate ligand is bonded to the Mo(1) centre in a planar fashion involving the *xy*-plane, coordinating through the phenolate oxygen O(4), the enolate oxygen O(1), the imine nitrogen atom N(2), and an oxo group O(5) lying *trans* to N(2). The fifth and sixth positions of the distorted octahedron are occupied by the bridging oxygen O(6) and the O atoms of the free ethanol molecule, respectively. The coordination around the Mo(2) centre is the same except that the sixth position is occupied by an oxo group O(8). The Mo(1)–O(9) (alcohol) bond [2.272(3) Å] is significantly longer than the other Mo(1)–O bonds [1.692(3)–2.029(2) Å] indicating that the alcohol molecule is weakly bonded to the MoO_2^{2+} core. The other bond lengths and bond angles in the organic ligands are close to standard values [62]. In the crystal of complex **2**, molecules are bridged by O–H···O hydrogen bonds (dashed lines, Fig. 5) involving the coordinated and solvent molecules of ethanol, forming chains propagating along the *c* axis direction. Details of the classical hydrogen bonding in complex **2** are given in Table 6.

3.5. Inhibition of cancer cell viability

In the present study antiproliferative efficacy of complexes **1** and **2** was assayed by determining the viability of HeLa cells using the MTT assay method. The salicyloylhydrazide and $MoO_2(acac)_2$ gave high IC_{50} values of >200 μM, whereas **1** and **2** gave values in the range 33–28 μM. In contrast, cisplatin, gefitinib, gemcitabine, 5-fluorouracil and vinorelbine, the most commonly used chemotherapeutic drugs, are comparably effective in HeLa cells with an IC_{50} value of 13, 20, 35, 40 and 48 μM, respectively under similar experimental conditions [63]. The significant decrease in the inhibitory concentration for the ligand compared to the metal

Table 6
Hydrogen bond distances (A) and angles (°) for complex **2**.

D–H···A	D–H (Å)	H···A (Å)	D···A (Å)	∠D–H···A (°)
O9–H90...O10	0.811(19)	1.81(2)	2.601(4)	163(5)
O10–H100...O4	0.82	2.27	2.988(4)	147
O10–H100...O9	0.82	2.49	3.189(4)	143

Symmetry transformations used to generate equivalent atoms: (a) $-x$, $-y$, $-z+2$.

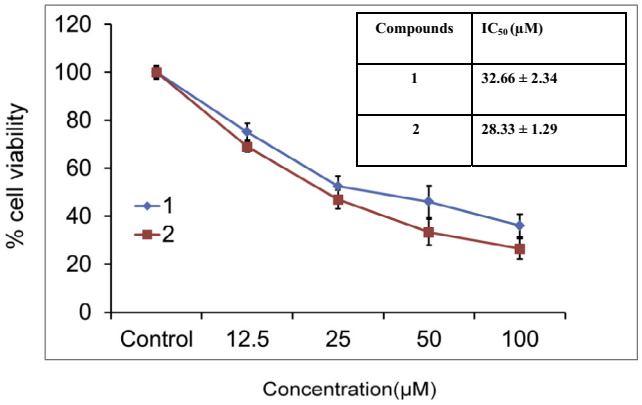

Fig. 6. Effect of complexes **1** and **2** on cell viability and growth. HeLa cells were treated with different concentrations of the test compounds for 72 h and then cell viability was measured by MTT assay. Data reported as the mean ± S.D. for $n = 6$ and compared against control by using a Student's *t*-test. (*Significant compared to control).

complex clearly indicates that incorporation of molybdenum in the ligand environment has a marked effect on cytotoxicity. A possible explanation is that by coordination the polarity of the ligand and the central metal ion are reduced through the charge equilibration, which favors permeation of the complexes through the lipid layer of the cell membrane [64,65]. The present results are consistent with the observation that metal complexes can exhibit greater biological activities than the free ligand [8].

Comparing the antiproliferative activity of two complexes, the cytotoxicity follows the order **2** > **1**, which is reflected from their IC_{50} values with dose dependency illustrated in Fig. 6. The inhibitory rate of **2** against HeLa cells is higher than **1**, which may be due to the presence of coordinated ethanol [66] and two bridging oxygen. Very recently the antiproliferative activity of some di and tri- oxomolybdenum(VI) compounds has been reported by Feng et al. using the similar technique against six different human cancer cell lines, i.e. A-549 (lung cancer), Bel-7402 (liver cancer), HCT-8 (colon cancer), BCG-832 (gastric cancer), HL (leukemia), and KB (nasopharyngeal), and the present results are in accordance with the reported values [67].

3.6. Nuclear staining assay

To examine the apoptotic potential of test compounds in HeLa cells, DAPI staining was done. Chromatin condensation that occurs during apoptosis (type I programmed cell death) is a characterizing marker of nuclear alteration. HeLa cells were treated with 30 and 25 μM of **1** and **2** respectively. All the doses were given below the calculated IC_{50} and the cells were incubated for 24 h before DAPI nuclear staining assay. Control cells (treated with 90% DMF) hardly showed any sort of condensation in comparison to the test compound's treated groups (as shown in Fig. 7), when the cells were examined under fluorescent microscope, DAPI filter. All images taken in grayscale demonstrate the brightly condensed chromatin bodies and the nuclear blebbings as marked by arrows in the figure. The drug treated groups besides showing nuclear changes also revealed a shrinking morphology – another important hallmark of apoptosis.

4. Conclusions

Two novel and unusual dimeric $[(Mo^{VI}O_2)_2L]$ (**1**) and tetrameric $[\{(C_2H_5OH)LO_3Mo_2^{VI}\}_2(\mu\text{-}O)_2]\cdot C_2H_5OH$ (**2**) oxidomolybdenum(VI) complexes with *N*,*N*′-disalicyloylhydrazine have been synthesized

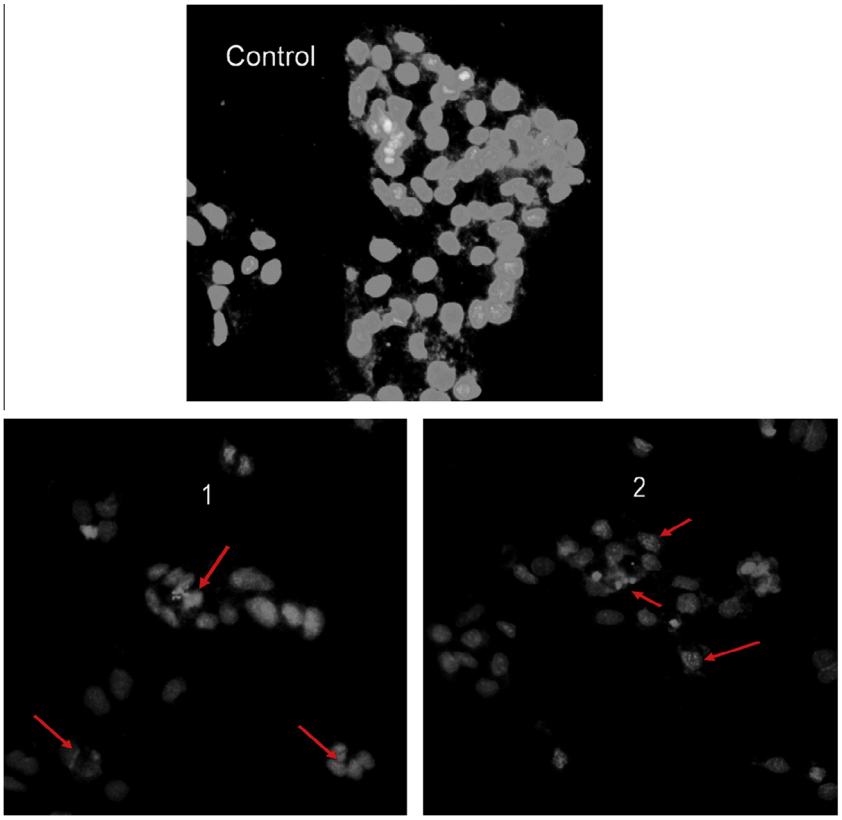

Fig. 7. Study of apoptosis by morphological changes in nuclei of HeLa cells. After treatment HeLa cells from control and treated group were fixed with 3.7% para formaldehyde for 15 min, permeabilized with 0.1% Triton X-100 and stained with 1 μg/ml DAPI for 5 min at 37 °C. The cellswere then washed with PBS and examined by fluorescence microscopy (Olympus IX 71) (200×).

and fully characterized. The binucleating ligand was formed by the self combination of hydrazine or corresponding hydrazone. The complexes were characterized by various spectroscopic techniques (IR, UV–Vis and NMR) and also by electrochemical study. The molecular structures of both have been confirmed by X-ray crystallography. The above studies indicate that the *N*,*N*′-disalicyloylhydrazine (H_2L) has the normal tendency to form both dimeric and tetrameric complexes coordinated through the dianionic tridentate manner. The *in vitro* antiproliferative activity of complexes **1** and **2** against HeLa cell line was assayed. Form the IC_{50} values (Fig. 6), complex **2** showed better cytotoxic activity though it has tetrameric structure which may be due to the presence of coordinated ethanol molecule [66] and di-μ-oxido type complex.

Acknowledgements

The authors thank the reviewers for their comments and suggestions, which were helpful in preparing the revised version of the manuscript. Funding for this research was provided by CSIR, Government of India (Grant No. 01(2735)/13/EMR-II). We acknowledge the use of UV–Vis spectrophotometer purchased from a DST (India) Grant No. SR/FT/CS-016/2008. Employing of the instrument Bruker SMART APEX II CCD diffractometer, from IACS, Kolkata, India, is sincerely acknowledged. S. Pasayat gratefully acknowledges the Council of Scientific and Industrial Research, New Delhi, India, for the award of research fellowship.

Appendix A. Supplementary data

CCDC 972688 and 972689 contain the supplementary crystallographic data for complex **1** and complex **2** respectively. These data can be obtained free of charge via http://www.ccdc.cam.ac.uk/conts/retrieving.html, or from the Cambridge Crystallographic Data Centre, 12 Union Road, Cambridge CB2 1EZ, UK; fax: (+44) 1223-336-033; or e-mail: deposit@ccdc.cam.ac.uk.

References

[1] M.J. Romao, M. Archer, I. Moura, J.J.G. Moura, J. LeGall, R. Engh, M. Schneider, P. Hof, R. Huber, Science 270 (1995) 1170.
[2] S.P. Kramer, J.L. Johnson, A.A. Ribiero, D.S. Millington, K.V. Rajagopalan, J. Biol. Chem. 262 (1987) 16357.
[3] D.B. Lovejoy, D.R. Richardson, Blood 100 (2002) 666.
[4] N. Farrell, Coord. Chem. Rev. 232 (2002) 1.
[5] B. Rosenberg, L.V. Camp, J.E. Trosko, V.H. Mansour, Nature 222 (1969) 385.
[6] C. Orvig, M. Abrams, J. Chem. Rev. 99 (1999) 2201.
[7] H. Sakurai, Y. Kojima, Y. Yoshikawa, K. Kawabe, H. Yasui, Coord. Chem. Rev. 226 (2002) 187.
[8] T. Rosu, E. Pahontu, S. Pasculescu, R. Georgescu, N. Stanica, A. Curaj, A. Popescu, M. Leabu, Eur. J. Med. Chem. 45 (2010) 1627.
[9] S. Padhye, Z. Afrasiabi, E. Sinn, J. Fok, K. Mehta, N. Rath, Inorg. Chem. 44 (2005) 1154.
[10] D. Kovala-Demertzi, A. Papageorgiou, L. Papathanasis, A. Alexandratos, P. Dalezis, J.R. Miller, M.A. Demertzis, Eur. J. Med. Chem. 44 (2009) 1296.
[11] V. Vrdoljak, I. Đilović, M. Rubčić, S.K. Pavelić, M. Kralj, D. Matković-Čalogović, I. Piantanida, P. Novak, A. Rožman, M. Cindrić, Eur. J. Med. Chem. 45 (2010) 38.
[12] T. Yamase, Mol. Eng. 3 (1993) 241.
[13] M. Cindrić, T.K. Novak, S. Kraljević, M. Kralj, B. Kamenar, Inorg. Chim. Acta 359 (2006) 1673.
[14] M.S. Saraiva, S. Quintal, F.C.M. Portugal, T.A. Lopes, V. Félix, J.M.F. Nogueira, M. Meireles, M.G.B. Drew, M.J. Calhorda, J. Org. Chem. 693 (2008) 3411.
[15] H. Thomadaki, A. Karaliota, C. Litos, A. Scorilas, J. Med. Chem. 50 (2007) 1316.
[16] D. Bandarra, M. Lopes, T. Lopes, J. Almeida, M.S. Saraiva, M. Vasconcellos-Dias, C.D. Nunes, V. Félix, P. Brandão, P.D. Vaz, M. Meireles, M.J. Calhorda, J. Inorg. Biochem. 104 (2010) 1171.
[17] B. Gleeson, J. Claffey, A. Deally, M. Hogan, L.M.M. Mendez, H. Muller-Bunz, S. Patil, M. Tacke, Inorg. Chim. Acta 363 (2010) 1831.
[18] L.H.A. Terra, M.C. Areias, I. Gaubeur, M.E.V. Suez-Iha, Spectrosc. Lett. 32 (1999) 257.
[19] M.R. Maurya, S. Agarwal, M. Abid, A. Azam, C. Bader, M. Ebel, D. Rehder, Dalton Trans. (2006) 937.
[20] L. Savini, L. Chiasserini, V. Travagli, C. Pellerano, E. Novellino, Eur. J. Med. Chem. 39 (2004) 113.
[21] Z. Cui, X. Yang, Y. Shi, H. Uzawa, J. Cui, H. Dohi, Y. Nishida, Bioorg. Med. Chem. Lett. 21 (2011) 7193.
[22] A.C. Cunha, J.M. Figueiredo, J.L.M. Tributino, A.L.P. Miranda, H.C. Castro, R.B. Zingali, C.A.M. Fraga, M.C.B.V. Souza, V.F. Ferreira, E. Barreiro, J. Bioorg. Med. Chem. 11 (2003) 2051.
[23] J. Easmon, G. Puerstinger, K.-S. Thies, G. Heinisch, J. Hofmann, J. Med. Chem. 49 (2006) 6343.
[24] T.B. Chaston, R.N. Watts, J. Yuan, D.R. Richardson, Clin. Cancer Res. 10 (2004) 7365.
[25] G.R. Braslawsky, M.A. Edson, W. Pearce, T. Kaneko, R.S. Greenfield, Cancer Res. 50 (1990) 6608.
[26] C.D. Fan, H. Su, J. Zhao, B.X. Zhao, S.L. Zhang, J.Y. Miao, Eur. J. Med. Chem. 45 (2010) 1438.
[27] Y. Xia, C.D. Fan, B.X. Zhao, J. Zhao, D.S. Shin, J.Y. Miao, Eur. J. Med. Chem. 43 (2008) 2347.
[28] K. Effenberger, S. Breyer, R. Schobert, Eur. J. Med. Chem. 45 (2010) 1947.
[29] F.F. Tian, J.H. Li, F.L. Jiang, X.L. Han, C. Xiang, Y.S. Ge, L.L. Li, Y. Liu, RSC Adv. 2 (2012) 501.
[30] S. Pasayat, S.P. Dash, S. Roy, R. Dinda, S. Dhaka, M.R. Maurya, W. Kaminsky, Y.P. Patil, M. Nethaji, Polyhedron 67 (2014) 1.
[31] M. Bagherzadeh, M. Zare, V. Amani, A. Ellern, L.K. Woo, Polyhedron 53 (2013) 223.
[32] X. He, J. Coord. Chem. 66 (2013) 966.
[33] S. Pasayat, S.P. Dash, Saswati, P.K. Majhi, Y.P. Patil, M. Nethaji, H.R. Dash, S. Das, R. Dinda, Polyhedron 38 (2012) 198.
[34] Y. Lei, C. Fu, Russ. J. Coord. Chem. 38 (2012) 65.
[35] N.K. Ngan, K.M. Lo, C.S.R. Wong, Polyhedron 33 (2012) 235.
[36] Y. Yamashita, M.M. Salter, K. Aoyama, S. Kobayashi, Angew. Chem., Int. Ed. 45 (2006) 3816.
[37] V.F. Shuĭgin, E.A. Sarnit, O.V. Konnik, E.B. Rusanov, A.S. Bogomyakov, V.I. Ovcharenko, V.V. Minin, Russ. J. Coord. Chem. 38 (2012) 44.
[38] Y.-T. Chen, D.-C. Li, Acta Crystallogr. 64 (2008) 1466.
[39] P.V. Bernhardt, P. Chin, P.C. Sharpe, J.C. Wang, D.R. Richardson, J. Biol. Inorg. Chem. 10 (2005) 761.
[40] J.M. Dou, M.L. Liu, D.C. Li, D.Q. Wang, Eur. J. Inorg. Chem. 23 (2006) 4866.
[41] D. Li, S. Wang, H. Xu, Y. Yang, S. Zeng, J. Zhao, D. Wang, J. Dou, Inorg. Chim. Acta 365 (2011) 85.
[42] R.P. John, J. Park, D. Moon, K. Lee, M.S. Lah, Chem. Commun. (2006) 3699.
[43] J.K. Daniel, N.P. Peet, J. Heterocycl. Chem. 15 (1978) 1309.
[44] H.H. Fox, J.T. Gibas, J. Org. Chem. 18 (1953) 1375.
[45] W. Von Gentzkow, H. Formanek, I. Dietrich, E. Knapek, Siemens Forsch.-Entwicklungsber 12 (1983) 149.
[46] S.R. Tewari, S.K. Bajpai, S.K. Misra, G.N. Shukla, V.N. Misra, J. Indian Chem. Soc. 59 (1983) 891.
[47] H. Zhao, N. Neamati, S. Sunder, H. Hong, S. Wang, G.W.A. Milne, Y. Pommier, T.R. Burke Jr., J. Med. Chem. 40 (1997) 937.
[48] S.P. Dash, S. Pasayat, S. Bhakat, S. Roy, R. Dinda, E. Tiekink, S. Mukhopadhyay, S. Bhutia, Manasi Hardikar, B. Joshi, Y.P. Patil, M. Nethaji, Inorg. Chem. (ASAP article) doi:10.1021/ic401866x.
[49] G.J.-J. Chen, J.W. McDonald, W.E. Newton, Inorg. Chem. 15 (1976) 2612.
[50] E.H. Rodd, in: Chemistry of Carbon Compounds, vol. 3, Elsevier, London, 1954, p. 556.
[51] R. Dinda, P. Sengupta, S. Ghosh, W.S. Sheldrick, Eur. J. Inorg. Chem. (2003) 363.
[52] A. Sarkar, S. Pal, Inorg. Chim. Acta 362 (2009) 3807.
[53] G.M. Sheldrick, Acta Crystallogr., Sect. A 64 (2008) 112.
[54] C.F. Macrae, I.J. Bruno, J.A. Chisholm, P.R. Edgington, P. McCabe, E. Pidcock, L. Rodriguez-Monge, R. Taylor, J. van de Streek, P.A.J. Wood, Appl. Crystallogr. 41 (2008) 466.
[55] S.K. Bhutia, S.K. Mallick, S.M. Stevens, L. Prokai, J.K. Vishwanatha, T.K. Maiti, Toxicol. In Vitro 22 (2008) 344.
[56] S.K. Bhutia, S.K. Mallick, S. Maiti, T.K. Maiti, Chem. Biol. Interact. 174 (2008) 11.
[57] B. Kwak, H. Rhee, M.S. Lah, Polyhedron 19 (2000) 1985.
[58] R.P. John, K. Lee, B.J. Kim, B.J. Suh, H. Rhee, M.S. Lah, Inorg. Chem. 44 (2005) 7109.
[59] S.K. Dutta, D.B. McConville, W.J. Youngs, M. Chaudhury, Inorg. Chem. 36 (1997) 2517.
[60] C.C.L. Pereira, S.S. Balula, F.A. AlmeidaPaz, A.A. Valente, M. Pillinger, J. Klinowski, I.S. Goucalves, Inorg. Chem. Commun. 46 (2007) 8508.
[61] S.F. Gheller, W.E. Newton, L.P. de Majid, J.R. Bradbury, F.A. Schultz, Inorg. Chem. 27 (1988) 359.
[62] F.H. Allen, O. Kennard, D.G. Watson, J. Chem. Soc., Perkin Trans. 12 (1987) 1.
[63] M. Ahmed, K. Jamil, Biol. Med. 3 (2011) 60.
[64] A.M. Ramadan, J. Inorg. Biochem. 65 (1997) 183.
[65] P.G. Avaji, C.H.V. Kumar, S.A. Patil, K.N. Shivananda, C. Nagaraju, Eur. J. Med. Chem. 44 (2009) 3552.
[66] D.S. Raja, G. Paramaguru, N.S.P. Bhuvanesh, J.H. Reibenspies, R. Renganathan, K. Natarajan, Dalton Trans. 40 (2011) 4548.
[67] J. Feng, X. Lu, G. Wang, S. Du, Y. Cheng, Dalton Trans. 41 (2012) 8697.